PNAS RESEARCH ARTICLE | BIOPHYSICS AND COMPUTATIONAL BIOLOGY OPEN ACCESS

Neutral lysophosphatidylcholine mediates α-synuclein-induced synaptic vesicle clustering

Ying Lai[a,b,1], Chunyu Zhao[c,1], Zhiqi Tian[d,1], Chuchu Wang[b,c,1], Jiaqi Fan[a,1], Xiao Hu[d], Jia Tu[c], Tihui Li[e], Jeremy Leitz[b], Richard A. Pfuetzner[b], Zhengtao Liu[c], Shengnan Zhang[c], Zhaoming Su[e], Jacqueline Burré[f], Dan Li[g], Thomas C. Südhof[b,h], Zheng-Jiang Zhu[c], Cong Liu[c,i,2], Axel T. Brunger[b,h,2], and Jiajie Diao[d,2]

Edited by James Hurley, University of California, Berkeley, CA; received June 21, 2023; accepted September 21, 2023

α-synuclein (α-Syn) is a presynaptic protein that is involved in Parkinson's and other neurodegenerative diseases and binds to negatively charged phospholipids. Previously, we reported that α-Syn clusters synthetic proteoliposomes that mimic synaptic vesicles. This vesicle-clustering activity depends on a specific interaction of α-Syn with anionic phospholipids. Here, we report that α-Syn surprisingly also interacts with the neutral phospholipid lysophosphatidylcholine (lysoPC). Even in the absence of anionic lipids, lysoPC facilitates α-Syn-induced vesicle clustering but has no effect on Ca^{2+}-triggered fusion in a single vesicle–vesicle fusion assay. The A30P mutant of α-Syn that causes familial Parkinson disease has a reduced affinity to lysoPC and does not induce vesicle clustering. Taken together, the α-Syn–lysoPC interaction may play a role in α-Syn function.

single molecule | synaptic vesicle | SNARE | α-synuclein | membrane

α-synuclein (α-Syn) is an abundant presynaptic protein that is expressed throughout the central nervous system and that is associated with synaptic vesicles (1–3). Despite evidence that α-Syn plays a role in neurodegenerative diseases (4), its physiological function in the healthy brain remains unclear. At a molecular level, α-Syn promotes SNARE-complex assembly at the synapse via binding to the SNARE protein synaptobrevin-2 (also called VAMP2, vesicle-associated membrane protein 2) and to phospholipids (5). Moreover, previously, we observed that α-Syn clusters proteoliposomes that mimic synaptic vesicles (6). This vesicle-clustering activity occurs for both recombinant α-Syn as well as for native α-Syn purified from mouse brains. We speculated that the clustering activity of α-Syn leads to an accumulation of synaptic vesicles at the active zone, which could promote neuronal trans-SNARE complex formation and provide a "buffer" of synaptic vesicles. Subsequent studies supported the notion of α-Syn-induced synaptic vesicle clustering in presynaptic boutons (7, 8).

α-Syn binds to a variety of lipid molecules, including glycerophospholipids, PUFA, and sphingolipids (9–11). More specifically, α-Syn interacts with anionic lipids through its N-terminal region (12). In our previous study, we only tested glycerophospholipids for a potential role in synaptic vesicle clustering and found that anionic glycerophospholipids (in particular, phosphatidylserine, PS), but not neutral glycerophospholipid (in particular, phosphatidylcholine, PC) or slightly positive charged (phosphatidylethanolamine, PE), mediate α-Syn-dependent SV clustering (6). On the other hand, anionic glyercophospholipids promote α-Syn aggregation at low lipid/α-Syn ratios (13, 14), suggesting a potential role of these lipid interactions in α-Syn pathology. We therefore reinvestigated whether other lipid molecules may also mediate synaptic vesicle clustering by α-Syn. Among possible candidates, here, we investigate the possible role of the neutral phospholipid lysophosphatidylcholine (lysoPC) since its unique one-tail structure may enhance membrane packing defects to induce an unexpected interaction with α-Syn.

Definitions

v-Vesicle. Proteoliposome with reconstituted synaptobrevin-2 (but not synaptotagmin-1) used for vesicle clustering experiments. The lipid composition was 59 mol% PC, 20 mol% PE, and 20 mol% cholesterol, and 1 mol% DiD or DiI dye, while 5 mol% lysoPC was used to substitute normal PC for lysoPC case. For the clustering experiments, 0.5 mol% lysoPC and 63.5 mol% PC were used. The v-vesicles were prepared as previously described (15).

SV-Vesicle. Proteoliposome with reconstituted synaptobrevin-2 and synaptotagmin-1 that mimics synaptic vesicles (SV). The lipid composition was 60 mol% PC, 20 mol% PE, and 20 mol% cholesterol, while 5 mol% lysoPC was used to substitute normal PC for lysoPC case. The SV-vesicles were prepared as previously described (15).

Significance

The previously identified interaction between α-Syn and negatively charged membranes alters the function and dynamics of α-Syn in neurons, while a neutral membrane has a negligible effect on α-Syn due to the lack of a strong interaction. The interaction between α-Syn and neutral lysoPC promotes synaptic vesicle clustering, and it may regulate the function and conformational dynamics of α-Syn in neurons.

Author affiliations: [a]National Clinical Research Center for Geriatrics, West China Hospital, State Key Laboratory of Biotherapy and Collaborative Innovation Center of Biotherapy, Sichuan University, Chengdu, Sichuan 610065, China; [b]Department of Molecular and Cellular Physiology, Stanford University, Palo Alto, CA 94305; [c]Interdisciplinary Research Center on Biology and Chemistry, Shanghai Institute of Organic Chemistry, Chinese Academy of Sciences, Shanghai 200032, China; [d]Department of Cancer Biology, University of Cincinnati College of Medicine, Cincinnati, OH 45267; [e]State Key Laboratory of Biotherapy, West China Cryo-electron Microscopy Center, West China Hospital, Sichuan University, Chengdu, Sichuan 610065, China; [f]Brain and Mind Research Institute and Appel Institute for Alzheimer's Disease Research, Weill Cornell Medicine, New York, NY 10021; [g]Key Laboratory for the Genetics of Developmental and Neuropsychiatric Disorders (Ministry of Education), Bio-X Institutes, Shanghai Jiao Tong University, Shanghai 200230, China; [h]HHMI, Stanford University, Palo Alto, CA 94305; and [i]State Key Laboratory of Chemical Biology, Shanghai Institute of Organic Chemistry, Chinese Academy of Sciences, Shanghai 200032, China

Author contributions: C.L., A.T.B., and J.D. designed research; Y.L., C.Z., Z.T., C.W., J.F., X.H., J.T., T.L., J.L., R.A.P., and Z.L. performed research; C.L., A.T.B., and J.D. contributed new reagents/analytic tools; Y.L., C.Z., Z.T., C.W., J.F., X.H., J.T., S.Z., Z.S., and Z.-J.Z. analyzed data; and J.B., D.L., T.C.S., C.L., A.T.B., and J.D. wrote the paper.

The authors declare no competing interest.

This article is a PNAS Direct Submission.

[1]Y.L., C.Z., Z.T., C.W., and J.F. contributed equally to this work.

[2]To whom correspondence may be addressed. Email: liulab@sioc.ac.cn, brunger@stanford.edu, or jiajie.diao@uc.edu.

This article contains supporting information online at https://www.pnas.org/lookup/suppl/doi:10.1073/pnas.2310174120/-/DCSupplemental.

Published October 26, 2023.

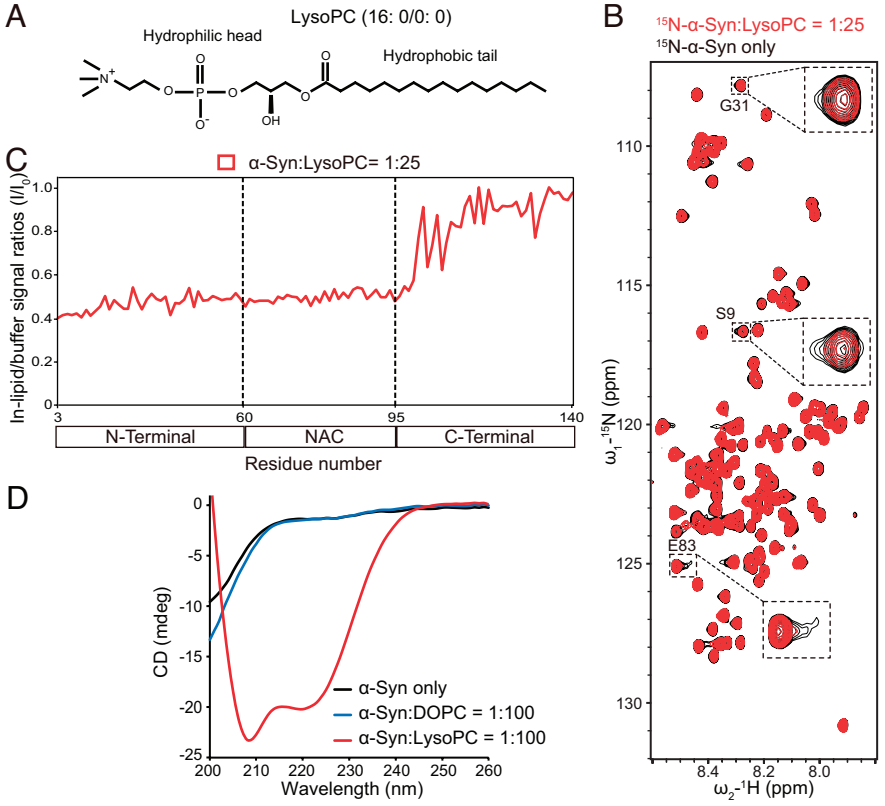

Fig. 1. α-Syn interacts with neutral lysoPC (*A*) Schematic diagram of lysoPC (16:0/0:0). Note that the main difference to PC is in the tail region. (*B*) 2D ^{1}H-^{15}N HSQC spectra of α-Syn titrated with lysoPC micelles at α-Syn/lysoPC molar ratio of 1:25. (*C*) Residue-resolved NMR signal intensity ratios (I/I_0) of WT α-Syn titrated by lysoPC (molar ratios of α-Syn/LysoPC is 1:25) to WT α-Syn alone. (*D*) CD spectra of α-Syn alone or α-Syn mixed with DOPC or lysoPC.

PM-Vesicle. Proteoliposome with reconstituted syntaxin-1A and SNAP-25A that mimics the plasma membrane (PM). The lipid composition was Brain Total Lipid Extract (Avanti Polar Lipids) supplemented with 3 mol% PIP2 and 0.1 mol% biotinylated PE. The PM-vesicles were prepared as previously described (15).

SV/PM-Vesicle Association. Number of SV-vesicles that bind to a surface with tethered PM-vesicles (*Materials and Methods*).

Results

Neutral LysoPC Interacts with α-Syn. LysoPC contains choline as a headgroup with exactly one fatty acid chain at the sn-2 position (Fig. 1*A*), and it is generated from hydrolysis of PC by phospholipase A2 (16). α-Syn interacts with lysoPC as assessed by solution nuclear magnetic resonance (NMR) spectroscopy and circular dichroism (CD). The 2D ^{1}H-^{15}N heteronuclear single-quantum coherence (HSQC) spectrum shows signal attenuation of the first ~96 residues of ^{15}N-labled α-Syn upon addition of pure lysoPC micelles, suggesting that the first ~96 residues of α-Syn are involved in lysoPC binding (Fig. 1 *B* and *C*). Moreover, lysoPC micelles induce α-helical structure in otherwise intrinsically disordered α-Syn monomers, similar to previous work that demonstrated induced structure by incubation with negatively charged lipid vesicles (13, 17), while, as a negative control, the addition of 1,2-dioleoyl-sn-glycero-3-phosphocholine (DOPC) liposomes showed no effect (Fig. 1*D*).

α-Syn–LysoPC Interaction Has No Effect on Ca^{2+}-Independent and Ca^{2+}-Triggered Membrane fusion. To assess a potential role of the α-Syn–lysoPC interaction in SV cycling, we tested whether it influences membrane fusion using a single vesicle–vesicle fusion assay with reconstituted synaptic proteins (18, 19) (Fig. 2*A*, *Definitions*). Free-floating "SV-vesicles" (with reconstituted synaptobrevin-2 and synaptotagmin-1) mimicked synaptic vesicles, while surface-tethered "PM-vesicles" (with reconstituted syntaxin-1A and SNAP-25A) mimicked the plasma membrane. A defined volume of SV-vesicle solution was incubated with PM-vesicles together with complexin-1, establishing a metastable state at zero Ca^{2+}. As a first step to assess the potential role of lysoPC on α-Syn function, we incorporated 5 mol% lysoPC into SV-vesicles during the preparation, while PS lipid was absent in contrast to our previous work (6) to eliminate any influence from negatively charged lipids. Previous studies estimated the lysoPC level in the blood plasma to be in the range of 200 to 400 μM (20–22), so our concentration of 5 mol% lysoPC falls into this range, assuming that lysoPC is incorporated into synaptic membranes at this concentration. Of course, this is an upper limit of the potential lysoPC concentration, and below we used a lower concentration as well. We tested the effect of recombinant α-Syn in our system by adding it during the SV-vesicle incubation stage. For the SV-vesicles that docked, we found that the α-Syn–lysoPC interaction had little effect on both Ca^{2+}-independent fusion even at this high lysoPC concentration (5 mol%) (Fig. 2*B*, note that the probabilities and amplitudes have been normalized by the number of associated vesicle–vesicle pairs) and on the efficiency and the kinetics of Ca^{2+}-triggered fusion upon injection of 500 μM Ca^{2+} (Fig. 2*C*).

LysoPC Facilitates Synaptic Vesicle Clustering Induced by α-Syn. We next tested whether the α-Syn–lysoPC interaction induces vesicle clustering using a single vesicle method as previously described (6) (Fig. 3*A*). In the presence of both α-Syn and lysoPC, we found a reduced number of SV-vesicles (again, without PS) that docked to surface-tethered PM-vesicles (Fig. 3*B*). In contrast to our previous results (6), PS lipids were absent in the SV-vesicles, and, as expected, α-Syn did not cause a difference in vesicle association for SV-vesicles without lysoPC. As a finite volume of SV-vesicles was used during the incubation stage, the decrease in SV/PM-vesicle pairs could be caused either by interference of SNARE-mediated SV/PM vesicle interactions or by affecting the number of available SV-vesicles by clustering. We therefore tested the effect

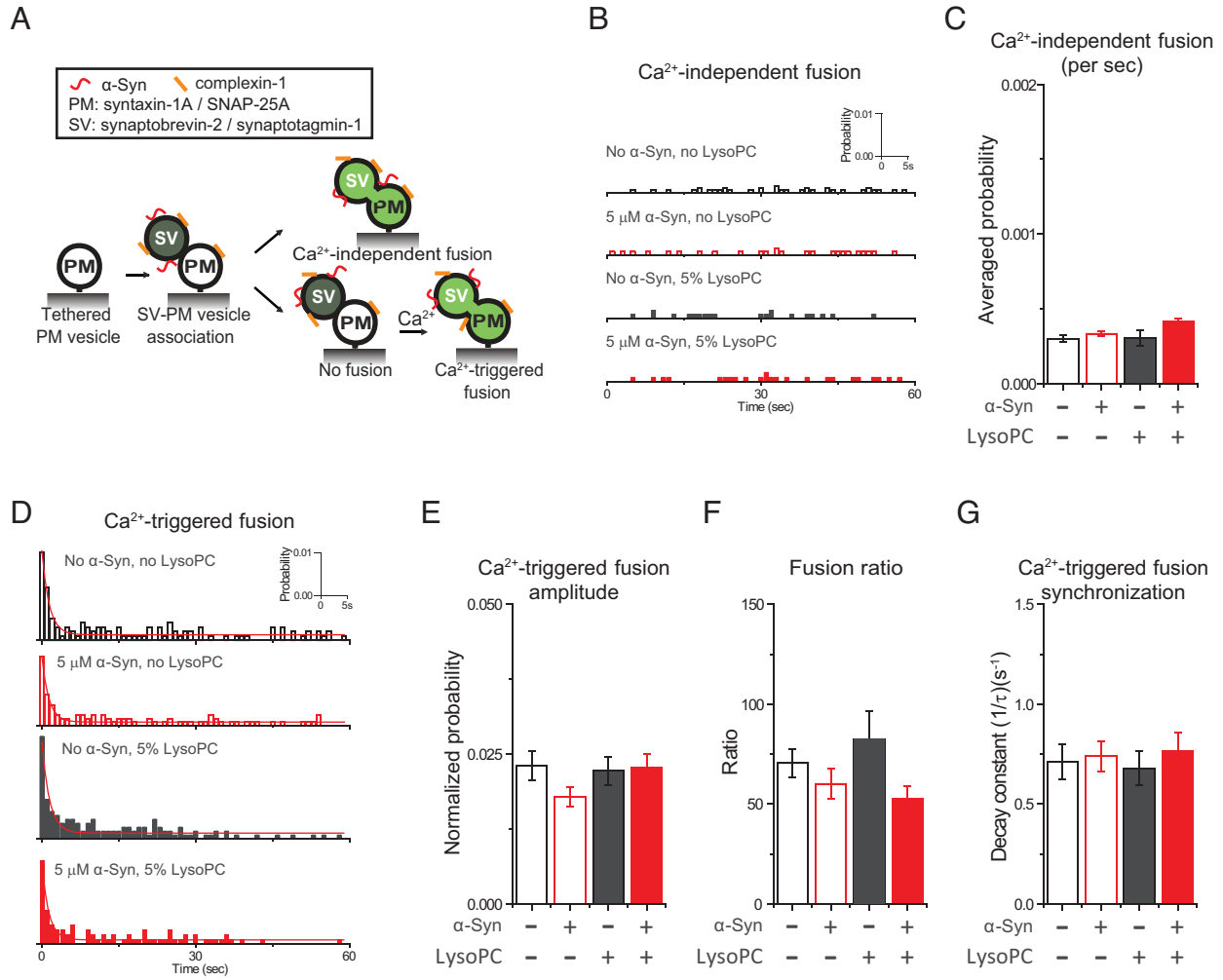

Fig. 2. The α-Syn-lysoPC interaction has no effect on SV/PM-vesicle fusion. (*A*) Experimental scheme of single-vesicle content-mixing system. (*B*) Effects of 5 μM α-Syn and 5% lysoPC on Ca^{2+}-independent fusion probabilities. (*C*) The bar graphs show the effect of 5 μM α-Syn and 5% lysoPC on the averaged probability of Ca^{2+}-independent fusion events. (*D*) Effects of 5 μM α-Syn and 5% lysoPC on Ca^{2+}-triggered fusion probabilities. (*E*–*G*) The bar graphs show the effect of 5 μM α-Syn and 5% lysoPC on normalized probability of Ca^{2+}-triggered fusion during the first 1-s time bin upon Ca^{2+}-injection (referred to as the Ca^{2+}-triggered amplitude) (*E*), the ratio of Ca^{2+}-triggered amplitude to the average probability of Ca^{2+}-independent fusion per second (*F*), and the decay rate of the histogram of fusion events upon 500 μM Ca^{2+}-injection (*G*). The probabilities and amplitudes were normalized by the number of associated SV/PM vesicle–vesicle pairs. Note that PS was absent in the preparations of the SV-vesicles in contrast to our previous work (6). Panels (*C*, *E*, and *F*) show means ± SEM for multiple independent repeat experiments (*SI Appendix*, Table S1). Decay constants and error estimates in panel *G* were computed from the covariance matrix upon fitting the corresponding histograms with a single exponential decay function using the Levenberg–Marquardt algorithm.

of the α-Syn–lysoPC interaction by measuring the interactions between vesicles of the same type: one population of v-vesicles (proteoliposomes with reconstituted synaptobrevin-2) labeled with 1% DiI (with reconstituted synaptobrevin-2) was tethered to an imaging surface while another population of v-vesicles labeled with DiD was freely diffusing in the sample chamber. Both vesicle populations were labeled with spectrally distinct fluorescent lipid analogues allowing tracking of the location of the free-floating vesicles and assessment of the surface coverage of the tethered vesicles. Interactions between both populations of v-vesicles were measured by counting the number of initially free-floating v-vesicles that bound to the tethered v-vesicles. We refer to this quantity as "clustering" between the same type vesicles (v/v-vesicle). Using this assay, we found that lysoPC significantly increases the number and the size of v-vesicle clusters induced by α-Syn (Fig. 3 *C* and *D*) in the absence of anionic lipids. By imaging the vesicles with cryogenic electron microscopy (Cryo-EM), we confirmed that the size difference of v-vesicles with or without lysoPC is negligible and that there are no changes in vesicle morphology (*SI Appendix*, Fig. S1). Furthermore, single-molecule binding measurements of Cy5-labeled α-Syn demonstrated that 5 mol% lysoPC enhances liposome binding of α-Syn (*SI Appendix*, Fig. S2). When we reduced the lysoPC levels to 0.5 mol%, we still observed α-Syn-induced v-vesicle clustering (Fig. 3*E*).

A30P Mutant Weakens α-Syn-Mediated Vesicle Clustering. Previously, we found that the Parkinson's disease (PD) familial A30P mutant of α-Syn (23) reduces the binding affinity to anionic PS or clustering of SV-vesicles (6). We further investigated the effect of the A30P mutant on the α-Syn–lysoPC interaction by NMR. Changes in signal intensity ratios in 2D ^{1}H-^{15}N HSQC spectra suggest that the A30P mutant disturbs the binding of the N terminus to lysoPC, especially for the first 35 residues (Fig. 4 *A* and *B*). Moreover, by impairing the binding to lysoPC, the A30P mutation diminished α-Syn-mediated vesicle clustering (Fig. 4*C*).

Discussion

Here, we found that in addition to anionic PS previously identified, neutral lysoPC at the concentrations tested in this work can bind to the N terminus of α-Syn and promote α-Syn-mediated SV

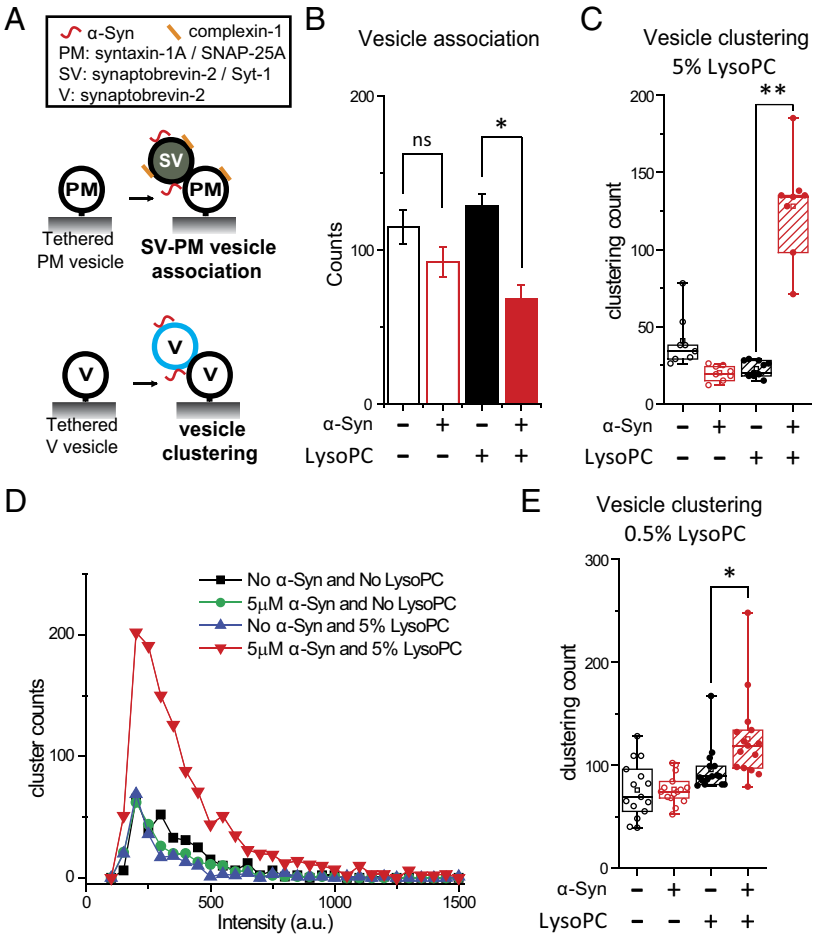

Fig. 3. LysoPC facilitates synaptic vesicle clustering induced by α-Syn. (*A*) Experimental scheme of single-vesicle docking and clustering assays. (*B*) α-Syn decreases the number of SV/PM-vesicle pairs. Shown is the number of SV-vesicles that were docked to immobilized PM-vesicles, in the presence of 2 μM complexin-1 and with or without 5 μM α-Syn or 5% lysoPC in SV-vesicles. (*C*) Purified recombinant α-Syn promotes v-vesicle clustering in the presence of lysoPC. α-Syn increases the number of interacting DiI-labeled v-vesicles on the imaging surface in a concentration-dependent manner. Shown are individual data points and box plots: The whiskers show the min and max values (excluding outliers), the box limits are the 25% and 75% percentiles, and the center line denotes the median. n = 10 to 12 random imaging locations in the sample channel obtained. $^{**}P < 0.01$ by Student's *t* test. (*D*) Distribution of the fluorescence intensity of all observed fluorescent spots for each of the four conditions, corresponding to the experiments shown in panel (*C*). The increase of the high-intensity population in the presence of α-Syn and lysoPC suggests the formation of large v-vesicle clusters. (*E*) Purified recombinant α-Syn promotes v-vesicle clustering in the presence of 0.5 mol% lysoPC. Note that PS was absent in the preparation of the SV- and v-vesicles in contrast to our previous work (6). Shown are individual data points and box plots as defined in panel (*C*). n = 15 random imaging locations in the sample channel were obtained, and $^{*}P < 0.05$ by the Student's *t* test.

clustering without affecting synaptic vesicle fusion. Furthermore, the PD-associated mutation A30P may disrupt the interaction with lysoPC as well as clustering.

In solution, α-Syn is a largely unfolded protein with a propensity to aggregate into β-sheet-rich amyloid-like fibrils in a nucleation-dependent manner, which contributes to the formation of Lewy bodies

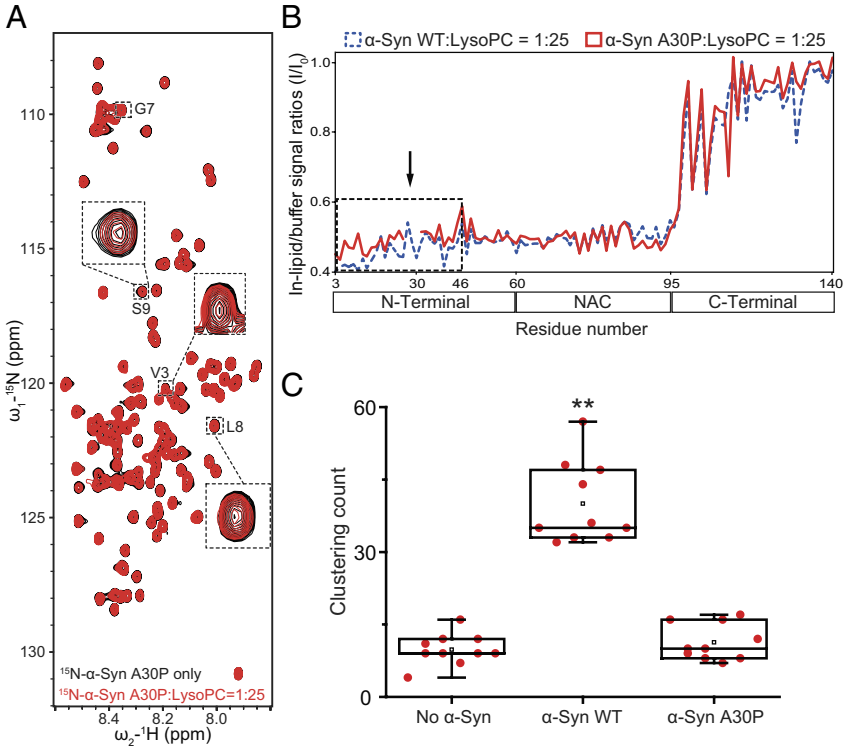

Fig. 4. The A30P mutation impairs lysoPC binding and abolishes α-Syn-mediated vesicle clustering. (*A*) 2D ^{1}H-^{15}N HSQC spectra of mutant (A30P) α-Syn in NMR buffer (black) and in the presence of lysoPC micelles at a protein/lipid molar ratio of 1:25 (blue). (*B*) Residue-resolved NMR signal intensity ratios (I/I0) of WT α-Syn and A30P mutant in the presence of lysoPC micelles at a protein/lipid molar ratio of 1:25. Note, that the signal of residue 30 is absent for the mutant A30P α-Syn. The dashed-line box highlights the region (amino acid residues 1 to 46) that shows a substantial difference. (*C*) Number of interactions between free-floating and tethered v-vesicles in the absence and presence of WT α-Syn and mutant (A30P) α-Syn using the single vesicle–vesicle clustering assay (*Materials and Methods*). Shown are individual data points and box plots. n = 10 random imaging locations in the sample channel were obtained, and $^{**}P < 0.01$ by the Student's *t* test.

(24). Therefore, intracellular factors such as proteins and membranes are critical to preserve the physiological conformation of α-Syn. As the most abundant lysophospholipid in the human body (25), lysoPC may play a role in maintaining functional α-Syn through an interaction with synaptic vesicles. As an inverted-cone-shape neutral lipid, lysoPC may introduce membrane curvature and membrane packing defects, which may impact membrane binding of α-Syn (26). However, we do not observe gross changes in membrane morphology at the lysoPC concentration tested here (*SI Appendix*, Fig. S1). Small packing defects may promote a hydrophobic interaction (27) between lysoPC and α-Syn which is distinct from electrostatically driven α-Syn–membrane interactions that accelerate aggregation at low lipid/α-Syn ratios (13, 14). This α-Syn–lysoPC interaction may regulate the function and conformational dynamics of α-Syn. Future work is required to explore the potential impact of lysoPC on pathological aggregation of α-Syn.

Materials and Methods

Recombinant SNAREs, Synaptotagmin-1, and Complexin-1 Expression and Purification. All proteins were from rat and expressed and purified as described by refs. 18, 19, and 28. Briefly, his-tagged syntaxin-1A, synaptobrevin-2, SNAP-25A, and synaptotagmin-1 were expressed in *Escherichia coli* and purified using a combination of Ni-NTA affinity (Qiagen) and size-exclusion chromatography on a Superdex 200 column (GE Healthcare). Synaptotagmin-1 was further purified using cation exchange chromatography on a Mono-S column (GE Healthcare). His-tags were removed from syntaxin-1A, synaptobrevin-2, and SNAP-25A with tobacco etch virus protease, or from synaptotagmin-1 with PreScission protease (GE Healthcare). Wildtype (WT) complexin-1 was purified essentially as described (18, 19, 28). All the proteins were flash-frozen and stored as aliquots at −80 °C.

Recombinant α-Syn Expression and Purification. α-Syn (full length) was cloned into the ampicillin-resistant bacterial expression vector pET22. BL21(DE3) competent cells were transformed with full-length plasmid and subsequently grown in LB media. Cell growth was carried out at 37 °C, 220 rpm to an OD600 of 0.6 to 0.8. Then, the expression of the protein was induced by 1 mM isopropyl-1-thio-D-galactopyranoside at 37 °C for 4 h. Bacteria were harvested by centrifugation and then resuspended and lysed in 100 mM Tris-HCl, pH 8.0, 1 mM ethylenedinitrilotetraacetic acid (EDTA), and 1 mM phenylmethylsulfonyl fluoride (PMSF). After centrifugation at 16,000 *g* for 30 min, the supernatants were heated for 10 min at 100 °C followed by centrifugation at 16,000 *g* for 30 min. Subsequently, streptomycin (20 mg/mL) was added to the supernatants. The mixture was then stirred on ice for 30 min and centrifuged at 16,000 *g* for 30 min. The pH value of supernatants was adjusted to 3.5 by 2 M HCl. Then, the supernatants were dialyzed into 25 mM Tris-HCl, pH 8.0, overnight at 4 °C after centrifugation at 16,000 *g* for 30 min. The dialyzed solution was loaded onto an anion exchange column (HiTrap Q FF, GE Healthcare) and eluted by a gradient of NaCl (0-1 M), followed by a size-exclusion chromatography (GE Healthcare, Superdex 75) in 25 mM Tris-HCl, pH 8.0.

CD Spectroscopy. Samples of 10 μM α-Syn incubated in the presence of increasing concentrations of lysoPC were measured by Chirascan (Applied Photophysics) at 25 °C. The baseline was corrected by sample buffer (25 mM Tris-HCl, pH 8.0). The path length of the quartz cuvettes was 0.5 mm. Each CD spectrum was obtained by averaging three spectra. The wavelength scans ranged from 260 nm to 200 nm with a scanning speed of 0.5 s/nm and a bandwidth of 1 nm. The CD signals of α-Syn measured at 222 nm were plotted as a function of lysoPC/α-Syn (molar ratios) which fit well to a single-step binding model.

NMR Spectroscopy. NMR experiments were carried out at 298 K on a Bruker 900 MHz spectrometer equipped with a cryogenic probe. ^{15}N-labeled WT and A30P α-Syn were prepared in "NMR buffer" of 50 mM sodium phosphate buffer and 50 mM NaCl at pH 6.5 with a concentration ~200 μM. LysoPC was prepared in the same NMR buffer at a concentration of 50 mM. 50 μM WT and A30P α-Syn were prepared in a final volume of 500 μL and 10 v/v% D_2O, respectively. After collecting protein-only 2D ^{1}H-^{15}N HSQC spectra in NMR buffer, 12.5 μL of the lysoPC was added into the NMR sample, and another HSQC spectra were collected. The Bruker standard pulse sequence hsqcetfpf3gpsi was used to collect the HSQC spectra, using two-dimensional complex dimensions of 2,048 and 200. All NMR data were processed using NMRPipe (29) and analyzed by SPARKY (30). Backbone resonance assignment of α-Syn was accomplished by using Biological Magnetic Resonance Bank (BMRB) entry 6968 (30).

Single Vesicle–Vesicle Content-Mixing Assay. The assay followed previously published protocols (31). Briefly, Surface passivation of quartz slides was performed by coating the surface with polyethylene glycol (PEG) molecules to eliminate nonspecific binding of vesicles. The same protocol and quality controls (surface coverage and nonspecific binding) were used as described previously (18, 19, 28). The surface was functionalized by inclusion of biotin-PEG during PEGgylation. A quartz slide was assembled into a flow chamber and incubated with NeutrAvidin (0.1 mg/mL). Biotinylated PM-vesicles (100× dilution) were tethered by incubation at room temperature (~25 °C) for 30 min, followed by three rounds of washing with 120 μL vesicle buffer in order to remove unbound PM-vesicles. Upon the start of illumination and recording of the fluorescence from a particular field of view of the flow chamber, SV-vesicles (diluted 100 to 1,000 times) were loaded into the flow chamber to directly monitor vesicle association of SV-vesicles to PM-vesicles for 1 min; when α-Syn was included in a particular experiment, it was added concurrently together with the SV-vesicles and 2 μM complexin. The lipid composition of SV-vesicles was 60 mol% phosphatidylcholine 1-palmitoyl-2-oleoyl-glycero-3-phosphocholine(POPC), 20 mol% 1,2-dioleoyl-sn-glycero-3-phosphoethanolamine (DOPE), and 20 mol% cholesterol, while 5 mol% lysoPC was used to substitute normal PC for lysoPC case. While continuing the recording, the flow chamber was washed three times with 120 μL of vesicle buffer including 2 μM complexin and 5 μM α-Syn in order to remove unbound SV-vesicles. Subsequently, we continued recording for another minute to monitor spontaneous fusion events. To initiate Ca^{2+}-triggered fusion events within the same field of view, a solution consisting of vesicle buffer, 500 μM Ca^{2+}, 500 nM Cy5 dye molecules as an indicator for the arrival of Ca^{2+}, 2 μM complexin, and 5 μM α-Syn was injected into the flow chamber. The injection was performed at a speed of 66 μl s^{-1} by a motorized syringe pump (Harvard Apparatus) using a withdrawal method.

All experiments were performed on a prism-type total internal reflection fluorescence (TIRF) microscope using 532 nm (green) laser (CrystaLaser, Reno, NV) excitation. Two observation channels were created by a 640 nm single-edge dichroic beamsplitter (FF640-FDi01-25×36, Shemrock, Rochester, NY): One channel was used for the fluorescence emission intensity of the content dyes and the other one for that of the Cy5 dyes that are part of the injected Ca^{2+}-solution. The two channels were recorded on two adjacent rectangular areas (45 × 90 μm^2) of an electron multiplying charged-coupled device (emCCD) camera (iXon+ DV 897E, Andor Technology USA). The imaging data were recorded with the smCamera software from Taekjip Ha's group at Johns Hopkins University. Our procedure resulted in a time series of images over a total of 3 min, consisting of the subsequent 1-min periods of vesicle association, spontaneous, and Ca^{2+}-triggered fusion, plus 5 s intervals for buffer exchanges.

Fluorescent spots in the content dye channel were detected, but only those spots were analyzed that showed exactly one stepwise increase during the vesicle association period; this procedure excludes SV-vesicles that were already docked during a previous round when performing repeat experiments using the same flow chamber. Stepwise increases in the fluorescence intensity time traces were automatically detected by the computer program described previously (32, 33) and manually checked to ensure correct performance of the automated procedure. Histograms for spontaneous and triggered fusion event occurrence were plotted with a time bin of 1 s and fitted to a single exponential decay function. The error bars in Figs. 2 and 3*A* were calculated as SDs from at least three independent experiments.

Single Vesicle–Vesicle Clustering Experiments. For the clustering experiments, the same protocol of vesicle preparation was used as for the single vesicle–vesicle fusion experiments described in the previous section. The lipid composition was 59 mol% POPC, 20 mol% DOPE, and 20 mol% cholesterol, and 1 mol% 1,1′-dioctadecyl-3,3,3′,3′-tetramethylindodicarbocyanine perchlorate, DiIC18(5) (DiD) or 1,1'-dioctadecyl-3,3,3',3'-tetramethylindocarbocyanine perchlorate, DiIC18(3) (DiI) dye, while 5 mol% lysoPC was used to substitute normal PC for lysoPC case. Specifically, a saturated layer of DiD-labeled synaptobrevin-2 containing v-vesicles was tethered on an imaging surface via biotin/neutravidin interactions. DiD-labeled synaptobrevin-2 v-vesicle was diluted 20×; 100 μL of the diluted vesicle solution was injected into the sample chamber and incubated for 30 min, followed by buffer exchange (200 μL vesicle buffer). We confirmed that the vesicle-covered surfaces

were saturated and produced a homogeneous distribution for each surface preparation with red laser excitation (633 nm) of the DiD-labeled tethered vesicles. As previously reported, more than 1,000 vesicles could be tethered with this method (34).

The tethered v-vesicle surface was incubated with 5 μM α-Syn or its mutants at the specified concentration for 30 min. DiI-labeled synaptobrevin-2 vesicles were prepared with our reconstitution protocol (35) and diluted 500×. Hundred microliter of diluted free-floating v-vesicle solution was injected into the sample chamber. After an incubation period of 60 min, unbound v-vesicles were removed by buffer exchange (2 × 200 μL vesicle buffer).

As stated above, sample slides with multiple channels were monitored in a wide-field TIR fluorescence microscope using an emCCD camera. The smCamera program from Taekjip Ha's lab was used for data acquisition and analysis. A specified number of images were taken at random locations within each channel on the quartz slide. Details regarding software, slide assembly, and imaging protocols are described in ref. 36. The number of v-/v-vesicle interactions (clustering) was determined by counting the number of DiI fluorescent spots from emission of DiI upon excitation at 532 nm. The counts were averaged over the specified number of images at random locations in each sample channel. This simple averaging procedure was possible since the surface coverage was homogeneous. For each set of comparisons between different conditions and/or mutants, the same protein preparations and surface preparations (quartz slide with tethered vesicles) were used, and the conditions were run in separate channels on the same slide; although there was some variation in absolute numbers of counts, the relative differences were statistically similar for different protein preparations.

Cryo-EM Sample Preparation. V-vesicles with or without 5 mol% lysoPC in this experiment were derived from the same vesicle composition as the single vesicle–vesicle clustering experiments described previously and incubated in vesicle buffer with or without 5 μM α-Syn for 2 h at room temperature. Then, a total of 3 μL of the vesicle solution was applied onto glow-discharged (50 s) 200-mesh R2/1 Quantifoil Cu grids. The grids were blotted for 2.5 s in 100% humidity with no blotting offset and rapidly frozen in liquid ethane using a Vitrobot MarkIV (Thermo Fisher).

Cryo-EM Sample Data Acquisition and Data Processing. The frozen grids of vesicle samples were loaded into a Talos Arctica (Thermo Fisher) operated at 200 kV, condenser lens aperture 50 μm, spot size 7. Microscope magnification was at 150,000× (corresponding to a calibrated sampling of 0.98Å per physical pixel). Micrographs were collected using EPU software on a Falcon3 direct electron camera (Thermo Fisher), operating in counting mode at a recording rate of 38 raw frames per second and a total exposure time of 40 s and total dose of 40 e−/Å2. Micrographs were lowpass filtered accordingly and displayed in EMAN2.31.

Single-Molecule Protein–Vesicle Binding Assay. The lipid composition was 59.4 mol% POPC, 20 mol% DOPE, and 20 mol% cholesterol, 0.1 mol% DiI dye, and 0.5 mol% biotin-PE, while 5 mol% lysoPC was used to substitute normal PC for lysoPC case. And the mixture was dried in a vacuum and was resuspended in vesicle buffer to result in a total lipid concentration of 10 mM. Protein-free unilamellar vesicles with the diameter of 100 nm were prepared by extrusion through polycarbonate filters (Avanti Polar Lipids).

DiI-labeled unilamellar vesicles were tethered on a surface through biotin–streptavidin coupling (36). Binding events between the vesicles and α-Syn A140C-Cy5 were monitored in real time at ambient temperature for 5 to 10 min right after 1 nM A140C-Cy5 was loaded with oxygen scavenger buffer (0.1 mg/mL glucose oxidase, 0.02 mg/mL catalase, 0.4 wt% β-D-glucose, and 0.1% cyclooctatetraene). Labeled α-Syn and liposomes were excited with red laser (635 nm) and green laser (532 nm) laser light, respectively. Images of both channels were acquired simultaneously using a dichroic beam splitter on an emCCD camera. For the data shown in *SI Appendix*, Fig. S2*C*, there were 351 or 597 binding events in the absence or presence of lysoPC, respectively.

Data, Materials, and Software Availability. All study data are included in the article and/or *SI Appendix*.

ACKNOWLEDGMENTS. C.L. thanks the support from the National Key R&D Program of China (2019YFE0120600) and the CAS Project for Young Scientists in Basic Research (YSBR-095); Y.L. thanks the support from the National Natural Science Foundation of China (31900688 and 32170686). This research was supported by the NIH (R01NS121077 to J.D. and J.B., R01NS102181, R01NS113960, 1RF1NS126342, and R21NS127939 to J.B., P50NS094733 and R01NS077906 to T.C.S., and R01MH063105 to A.T.B.).

1. L. Maroteaux, J. T. Campanelli, R. H. Scheller, Synuclein – a neuron-specific protein localized to the nucleus and presynaptic nerve-terminal. *J. Neurosci.* **8**, 2804–2815 (1988).
2. P. H. Jensen, M. S. Nielsen, R. Jakes, C. G. Dotti, M. Goedert, Binding of alpha-synuclein to brain vesicles is abolished by familial Parkinson's disease mutation. *J. Biol. Chem.* **273**, 26292–26294 (1998).
3. C. Wang *et al.*, Versatile structures of alpha-synuclein. *Front Mol. Neurosci.* **9**, 48 (2016).
4. M. Goedert, Alpha-synuclein and neurodegenerative diseases. *Nat. Rev. Neurosci.* **2**, 492–501 (2001).
5. J. Burre *et al.*, alpha-synuclein promotes SNARE-complex assembly in vivo and in vitro. *Science* **329**, 1663–1667 (2010).
6. J. Diao *et al.*, Native alpha-synuclein induces clustering of synaptic-vesicle mimics via binding to phospholipids and synaptobrevin-2/VAMP2. *Elife* **2**, e00592 (2013).
7. L. Wang *et al.*, alpha-synuclein multimers cluster synaptic vesicles and attenuate recycling. *Curr. Biol.* **24**, 2319–2326 (2014).
8. K. J. Vargas *et al.*, Synucleins have multiple effects on presynaptic architecture. *Cell Rep.* **18**, 161–173 (2017).
9. M. Zhu, J. Li, A. L. Fink, The association of alpha-synuclein with membranes affects bilayer structure, stability, and fibril formation. *J. Biol. Chem.* **278**, 40186–40197 (2003).
10. G. De Franceschi *et al.*, Molecular insights into the interaction between alpha-synuclein and docosahexaenoic acid. *J. Mol. Biol.* **394**, 94–107 (2009).
11. Y. V. Taguchi *et al.*, Glucosylsphingosine promotes alpha-synuclein pathology in mutant GBA-associated Parkinson's disease. *J. Neurosci.* **37**, 9617–9631 (2017).
12. E. Jo, J. McLaurin, C. M. Yip, P. St George-Hyslop, P. E. Fraser, alpha-Synuclein membrane interactions and lipid specificity. *J. Biol. Chem.* **275**, 34328–34334 (2000).
13. C. Galvagnion *et al.*, Lipid vesicles trigger alpha-synuclein aggregation by stimulating primary nucleation. *Nat. Chem. Biol.* **11**, 229–234 (2015).
14. M. Necula, C. N. Chirita, J. Kuret, Rapid anionic micelle-mediated alpha-synuclein fibrillization in vitro. *J. Biol. Chem.* **278**, 46674–46680 (2003).
15. M. J. Kyoung, Y. X. Zhang, J. J. Diao, S. Chu, A. T. Brunger, Studying calcium-triggered vesicle fusion in a single vesicle-vesicle content and lipid-mixing system. *Nat. Protocols* **8**, 1–16 (2013).
16. W. J. Brown, K. Chambers, A. Doody, Phospholipase A2 (PLA2) enzymes in membrane trafficking: Mediators of membrane shape and function. *Traffic* **4**, 214–221 (2003).
17. W. S. Davidson, A. Jonas, D. F. Clayton, J. M. George, Stabilization of alpha-synuclein secondary structure upon binding to synthetic membranes. *J. Biol. Chem.* **273**, 9443–9449 (1998).
18. Y. Lai *et al.*, Complexin inhibits spontaneous release and synchronizes Ca2+-triggered synaptic vesicle fusion by distinct mechanisms. *Elife* **3**, e03756 (2014).
19. Y. Lai *et al.*, N-terminal domain of complexin independently activates calcium-triggered fusion. *Proc. Natl. Acad. Sci. U.S.A.* **113**, E4698–E4707 (2016).
20. A. Takatera *et al.*, Quantification of lysophosphatidylcholines and phosphatidylcholines using liquid chromatography-tandem mass spectrometry in neonatal serum. *J. Chromatogr. B Anal. Technol. Biomed. Life Sci.* **838**, 31–36 (2006).
21. K. Raffelt *et al.*, Systemic alterations in phospholipid concentrations of blood plasma in patients with thyroid carcinoma: An in-vitro (31)P high-resolution NMR study. *NMR Biomed.* **13**, 8–13 (2000).
22. M. Kuliszkiewicz-Janus, M. A. Tuz, S. Baczyński, Application of 31P MRS to the analysis of phospholipid changes in plasma of patients with acute leukemia. *Biochim. Biophys. Acta* **1737**, 11–15 (2005).
23. R. Kruger *et al.*, Ala30Pro mutation in the gene encoding alpha-synuclein in Parkinson's disease. *Nat. Genetics* **18**, 106–108 (1998).
24. L. C. Serpell, J. Berriman, R. Jakes, M. Goedert, R. A. Crowther, Fiber diffraction of synthetic alpha-synuclein filaments shows amyloid-like cross-beta conformation. *Proc. Natl. Acad. Sci. U.S.A.* **97**, 4897–4902 (2000).
25. M. Ishikawa *et al.*, Plasma and serum lipidomics of healthy white adults shows characteristic profiles by subjects' gender and age. *Plos One* **9**, e91806 (2014).
26. E. R. Middleton, E. Rhoades, Effects of curvature and composition on alpha-synuclein binding to lipid vesicles. *Biophys. J.* **99**, 2279–2288 (2010).
27. J. Liu *et al.*, Membrane packing defects in synaptic vesicles recruit complexin and synuclein. *Phys. Chem. Chem. Phys.* **23**, 2117–2125 (2021).
28. J. Gong *et al.*, C-terminal domain of mammalian complexin-1 localizes to highly curved membranes. *Proc. Natl. Acad. Sci. U.S.A.* **113**, E7590–E7599 (2016).
29. F. Delaglio *et al.*, NMRPipe: A multidimensional spectral processing system based on UNIX pipes. *J. Biomol. NMR* **6**, 277–293 (1995).
30. W. Bermel *et al.*, Protonless NMR experiments for sequence-specific assignment of backbone nuclei in unfolded proteins. *J. Am. Chem. Soc.* **128**, 3918–3919 (2006).
31. Y. Lai *et al.*, Molecular mechanisms of synaptic vesicle priming by Munc13 and Munc18. *Neuron* **95**, 591–607.e510 (2017).
32. J. J. Diao, M. L. Zhao, Y. X. Zhang, M. Kyoung, A. T. Brunger, Studying protein-reconstituted proteoliposome fusion with content indicators in vitro. *Bioessays* **35**, 658–665 (2013).
33. Z. Tian *et al.*, Biochemical studies of membrane fusion at the single-particle level. *Prog. Lipid Res.* **73**, 92–100 (2019).
34. J. J. Diao *et al.*, Complexin-1 enhances the on-rate of vesicle docking via simultaneous SNARE and membrane interactions. *J. Am. Chem. Soc.* **135**, 15274–15277 (2013).
35. J. Diao *et al.*, Synaptic proteins promote calcium-triggered fast transition from point contact to full fusion. *Elife* **1**, e00109 (2012).
36. J. Diao *et al.*, A single vesicle-vesicle fusion assay for in vitro studies of SNAREs and accessory proteins. *Nat. Protoc.* **7**, 921–934 (2012).